2-7-2002

MEX-3 interacting proteins link cell polarity to asymmetric gene expression in Caenorhabditis elegans

Nancy N. Huang
Harvard University

Darcy E. Mootz
Harvard University

Albertha J. M. Walhout
University of Massachusetts Medical School

See next page for additional authors

MEX-3 interacting proteins link cell polarity to asymmetric gene expression in Caenorhabditis elegans

Authors
Nancy N. Huang, Darcy E. Mootz, Albertha J. M. Walhout, Marc Vidal, and Craig P. Hunter

Comments
At the time of publication, Albertha J. Marian Walhout was not yet affiliated with the University of Massachusetts Medical School.

Development 129, 747-759 (2002)
Printed in Great Britain © The Company of Biologists Limited 2002
DEV8907

MEX-3 interacting proteins link cell polarity to asymmetric gene expression in *Caenorhabditis elegans*

Nancy N. Huang[1], Darcy E. Mootz[1], Albertha J. M. Walhout[2], Marc Vidal[2] and Craig P. Hunter[1,*]

[1]Department of Molecular and Cellular Biology, Harvard University, Cambridge, MA 02138, USA
[2]Dana-Farber Cancer Institute and Department of Genetics, Harvard Medical School, Boston, MA 02115, USA
*Author for correspondence (e-mail: hunter@mcb.harvard.edu)

Accepted 9 November 2001

SUMMARY

The KH domain protein MEX-3 is central to the temporal and spatial control of PAL-1 expression in the *C. elegans* early embryo. PAL-1 is a Caudal-like homeodomain protein that is required to specify the fate of posterior blastomeres. While *pal-1* mRNA is present throughout the oocyte and early embryo, PAL-1 protein is expressed only in posterior blastomeres, starting at the four-cell stage. To better understand how PAL-1 expression is regulated temporally and spatially, we have identified MEX-3 interacting proteins (MIPs) and characterized in detail two that are required for the patterning of PAL-1 expression. RNA interference of MEX-6, a CCCH zinc-finger protein, or SPN-4, an RNA recognition motif protein, causes PAL-1 to be expressed in all four blastomeres starting at the four-cell stage. Genetic analysis of the interactions between these mip genes and the par genes, which provide polarity information in the early embryo, defines convergent genetic pathways that regulate MEX-3 stability and activity to control the spatial pattern of PAL-1 expression. These experiments suggest that *par-1* and *par-4* affect distinct processes. *par-1* is required for many aspects of embryonic polarity, including the restriction of MEX-3 and MEX-6 activity to the anterior blastomeres. We find that PAL-1 is not expressed in *par-1* mutants, because MEX-3 and MEX-6 remain active in the posterior blastomeres. The role of *par-4* is less well understood. Our analysis suggests that *par-4* is required to inactivate MEX-3 at the four-cell stage. Thus, PAL-1 is not expressed in *par-4* mutants because MEX-3 remains active in all blastomeres. We propose that MEX-6 and SPN-4 act with MEX-3 to translate the temporal and spatial information provided by the early acting *par* genes into the asymmetric expression of the cell fate determinant PAL-1.

Key words: *Caenorhabditis elegans*, Pattern formation, Polarity, RNA-binding protein, Translational control

INTRODUCTION

A central question in developmental biology is how cells first acquire polarity and then use that polarity to produce daughter cells with distinct patterns of gene expression. In *C. elegans*, the anteroposterior polarity of the zygote is determined by the position of the sperm pronucleus (Goldstein and Hird, 1996), which organizes a cortical and cytoplasmic rearrangement that leads to the asymmetric distribution of maternally supplied mRNAs and proteins before first cleavage (reviewed by Kemphues and Strome, 1997). Two broad classes of maternally expressed patterning genes have been identified in the *C. elegans* embryo: early acting polarity genes, which are required to establish or maintain embryonic polarity, and cell fate determinants, which act later to direct lineage-specific patterns of development (reviewed by Bowerman, 1998). Defects in polarity genes such as the par genes (partitioning defective) result in early and extensive polarity defects, including loss of asymmetry in cell size, cell cycle time, spindle orientation and distribution of cell fate determinants. Identified cell fate determinants include transcription factors and transmembrane receptors that are asymmetrically distributed among early blastomeres and are required to direct the differentiation of blastomere-specific cell lineages.

While it is known that *par* gene activity is required to polarize the zygote and enable the proper segregation of cell fate determinants, the mechanisms of action are poorly understood. For example, PAR-1 and PAR-4 are cortically localized serine/threonine kinases; however, none of their phosphorylation targets is known (Guo and Kemphues, 1995; Watts et al., 2000). Similarly, *par-3* and *par-6* encode conserved PDZ domain proteins that apparently form a protein complex localized to the anterior cortex (Etemad-Moghadam et al., 1995; Hung and Kemphues, 1999; Joberty et al., 2000; Lin et al., 2000). However, the mechanism by which this PAR-3/PAR-6 complex confers polarity information to downstream targets is largely unknown. We are interested in understanding how the PAR proteins direct the asymmetric distribution of maternally supplied cell fate determinants.

Considering that maternal factors act to define asymmetries before zygotic transcription begins, the *par*-dependent distribution of maternal gene activities must be regulated by a variety of post-transcriptional mechanisms, including differential stability of RNA or protein, asymmetric RNA or

protein localization, and control of mRNA translation. Based on the pleiotropy of the *par* polarity phenotypes, it is likely that the PAR proteins indirectly regulate the distribution of maternal determinants through intermediate regulators. One candidate intermediate regulator is the RNA-binding protein MEX-3, which regulates the asymmetric expression of maternally encoded PAL-1 protein (Draper et al., 1996; Hunter and Kenyon, 1996).

pal-1 encodes a Caudal-like homeodomain protein that is required to specify the fate of posterior blastomeres (Waring and Kenyon, 1990; Hunter and Kenyon, 1996). While *pal-1* mRNA is present throughout the oocyte and early embryo, PAL-1 protein is not detected until the four-cell stage and then is only detected in posterior blastomeres (Hunter and Kenyon, 1996). This temporal and spatial patterning of PAL-1 expression is dependant on MEX-3, which contains two KH domain RNA binding motifs originally identified in hnRNP K (Draper et al., 1996; Siomi et al., 1994). *mex-3* mutant hermaphrodites express PAL-1 in oocytes and all cells of their embryos, resulting in anterior-to-posterior homeotic transformations that are dependent on *pal-1* (Hunter and Kenyon, 1996). These results suggest that the primary function of *mex-3* in the early embryo is to repress PAL-1 expression. Indeed, MEX-3 localization is complementary to that of PAL-1. MEX-3 is present at high levels in mature oocytes, and one- and two-cell embryos, while at the four-cell stage, MEX-3 becomes enriched in anterior blastomeres relative to posterior blastomeres (Draper et al., 1996). Proper regulation of PAL-1 expression is also dependent on the *pal-1* 3′ UTR, which can confer *mex-3*-dependent repression on reporter RNAs (Hunter and Kenyon, 1996). These observations suggest that MEX-3 may directly repress PAL-1 translation.

Not surprisingly, MEX-3 localization and activity is dependent on *par* activity. In *par-1*, *par-4* and *par-3* mutant four-cell embryos, MEX-3 is present at high levels in all cells, indicating that activity of these par genes is required to restrict MEX-3 to the anterior (Draper et al., 1996; Bowerman et al., 1997). In *par-1* and *par-4* mutants, the presence of MEX-3 in all cells is coincident with failure to express PAL-1 in any cell, as would be expected if MEX-3 directly represses PAL-1 expression (Hunter and Kenyon, 1996; Bowerman et al., 1997). By contrast, four-cell *par-3* embryos express PAL-1 in zero, two or four cells, despite uniformly high levels of MEX-3 in all cells, indicating that the mere presence of MEX-3 at the four-cell stage is not sufficient to repress PAL-1 expression (Bowerman et al., 1997). Finally, *par-3* mutant embryos do not express PAL-1 before the four-cell stage, indicating that *par-3* activity is required for spatial but not temporal control of PAL-1 expression.

To explore further how MEX-3 translates the cell and embryonic polarity information provided by the par genes into the blastomere-specific pattern of PAL-1 expression, we analyzed *par; mex-3* double mutants. Our results suggest that *par* activity promotes PAL-1 expression by inhibiting *mex-3*. To better understand how *mex-3* activity is controlled, we identified and characterized two MEX-3 interacting proteins, MEX-6 and SPN-4, which are required to pattern PAL-1 expression. In addition to disrupting the pattern of PAL-1, inhibition of either gene by RNAi causes a unique terminal phenotype and has a distinct effect on MEX-3 expression levels. Investigation of genetic interactions between these genes and the par genes shows that *par-1* and *par-3* act upstream, providing polarity information that controls the spatial pattern of MEX-3 activity. By contrast, *par-4* appears to act independently of *par-1* and *par-3* to inactivate MEX-3 at the four-cell stage. We conclude from these analyses that *mex-3*, *mex-6* and *spn-4* integrate spatial and temporal information from different sources to pattern PAL-1 expression in the early embryo.

MATERIALS AND METHODS

Nematode strains and alleles

Nematodes were cultured using standard conditions (Brenner, 1974). The Bristol strain N2 was used as the standard wild-type strain. The following mutant strains and alleles were also used: DP132, *edIs6[unc119::GFP] IV*; EU1, *skn-1(zu67) IV/DnT1(IV;V)*; JJ462, *+/nT1 IV; pos-1(zu148) unc-42(e270)/nT1 V*; JJ1237, *mex-6(pk440)*; JJ1238, *unc-30(e191) mex-5(zu199) IV/nT1 (IV;V)*; JJ1244, *mex-6(pk440); unc-30(e191) mex-5(zu199) IV/nT1 (IV;V)*; KK184, *par-4(it47ts)V*; KK288, *rol-4(sc8) par-1(b274)IV/DnT1(IV;V)*; KK653, *par-3(it71) unc-32(e189)/qC1 dpy-19(e1259ts) glp-1(q339) III*; PD4251, *ccIs4251[myo-3::GFP] I; dpy-20(e1282) IV*; PD4790, *mIs12[myo-2::GFP] ?*; SU93, *jcIs1 [jam-1::GFP] IV*.

Embryos from homozygous mutant mothers are referred to as mutant embryos. All listed strains can be obtained from the *Caenorhabditis* Genetics Center, with the exception of KK653, which was kindly provided by Ken Kemphues.

RNAi

Sense and antisense single-stranded RNA was prepared from PCR products generated with primers that contained T7 and T3 RNA polymerase promoters and then annealed to produce double-stranded RNA (dsRNA). Hermaphrodites were injected with dsRNA and allowed to recover at 25°C for 16 or more hours before progeny were collected. Progeny from injected hermaphrodites are referred to as RNAi embryos. *mex-3*, *mex-6* and *spn-4* dsRNA was prepared from full-length cDNAs. *par-3* dsRNA was prepared from a PCR product corresponding to bases 1743-2341 of the 4413 bp *par-3*-coding region. At the time embryos were collected for all experiments, 99% (1539/1553) of *mex-6(RNAi)* embryos failed to hatch and 100% (1840/1843) of *spn-4(RNAi)* embryos failed to hatch.

Yeast two-hybrid screen

The yeast two-hybrid screen was conducted as described by Walhout and Vidal (Walhout and Vidal, 2001). Bases 10-634 of the 1248 bp *mex-3*-coding region, coding for half the protein and containing both KH domains, was fused to the *gal-4* DNA-binding domain (DB) and used as bait in the screen. All constructs containing the C terminal half of MEX-3 fused to DB resulted in activation of reporter genes in the absence of any interacting protein, precluding its use in the screen. Approximately 200,000 yeast colonies were screened, yielding 14 unique positives. Library inserts were amplified from yeast as described (Walhout and Vidal, 2001) with the modification that T3 or T7 RNA polymerase sites were added to the ends of the oligonucleotides.

Inexplicably, injection of K07H8.10 dsRNA produced variable results from different preparations of RNA from identical templates. Three different preparations of RNA corresponding to three different regions of the predicted gene produced an RNAi phenotype characterized by embryonic lethality and PAL-1 expression in all cells starting at the four-cell stage. Numerous RNA preparations from the same templates using the same RNA synthesis protocol failed to produce embryonic lethality. Attempts to remedy the variability by using different regions of the RNA were unsuccessful. Because of these difficulties, we were unable to complete analysis of K07H8.10.

We speculate that the variability between RNA preparations may be due to the extremely repetitive nature of the gene sequence, which may interfere with the formation of sufficiently long stretches of fully duplex double-stranded RNA.

Terminal phenotype analysis

Embryos fertilized 16 or more hours after injection were examined when uninjected control embryos had almost hatched. The following strains expressing tissue-specific GFP reporters (see nematode strains and alleles) were used to visualize the indicated tissue types: PD4251 (body wall muscle), SU93 (epidermis), PD4790 (pharyngeal muscle) and DP132 (neurons). Intestine was visualized by using polarizing optics to view intestinal cell-specific gut granules. Phenotypes were confirmed by differential interference contrast (DIC) microscopy of RNAi embryos from N2 worms. Representative embryos are shown but some variability in the terminal phenotype of *spn-4(RNAi)* embryos was observed. Specifically, *spn-4(RNAi)* embryos fertilized at later times after injection generally underwent less differentiation, most notably often failing to produce differentiated gut tissue.

Antibodies and immunostaining

PAL-1 immunostaining was performed as described (Hunter and Kenyon, 1996). Affinity purified anti-MEX-3 antibodies were prepared from the sera of rabbits immunized with full-length MEX-3::$(his)_6$. Embryos were permeabilized by freeze-cracking and fixed by immersion in –20°C methanol for 15 minutes, followed by –20°C acetone for 15 minutes. Slides were rinsed in phosphate-buffered saline with 0.1% Tween (PBSt) before anti-MEX-3 antibodies were applied (1:100 in 3% bovine serum albumin, Sigma A-9306). Slides were incubated overnight at 20°C and washed three times in PBSt before secondary antibody (Jackson Immunologicals) was applied.

MEX-3 intensity measurements

Optical sections of MEX-3-stained embryos were taken 1 μm apart on the *z* plane after a 0.4 second exposure using a DeltaVision microscope CCD camera (Applied Precision) and analyzed using softWoRx (Applied Precision) software. In no case was the camera saturated at this exposure setting. The center of each embryo was defined as the three contiguous sections with the highest Hoescht 33258 signal; all measurements were taken in all three center sections and then averaged. For each cell analyzed, raw MEX-3 intensity was measured from a circle of set diameter that contained the entire nucleus and that was fully enclosed by the cell membrane. A background measurement was taken a set distance away from the embryo in an area with no obvious cellular material and then subtracted from the raw MEX-3 intensity. Importantly, ABa and EMS lack MEX-3-containing P-granules in both wild-type and *spn-4(RNAi)* embryos, ensuring that we are only measuring cytoplasmic MEX-3. For comparison of ABa to EMS within the same type of embryo, measurements were taken for both cells from the same embryo. For comparison of *spn-4(RNAi)* cells with wild-type cells, an equal number of *spn-4(RNAi)* and wild-type embryos were analyzed from each experiment to minimize the effect of experiment to experiment variability. The two samples being compared were then subjected to Welch's approximate *t*-test, which is used to compare the means from two normal populations without assuming equal variances (Zar, 1999).

RESULTS

par-1 and *par-4* promote PAL-1 expression by inhibiting *mex-3*-mediated repression

Four previously identified genes, *mex-3*, *par-1*, *par-4* and *par-3*, are required to pattern PAL-1 expression (Hunter and Kenyon, 1996; Bowerman et al., 1997). To reveal aspects of the regulatory processes controlled by these proteins, we scored PAL-1 localization in oocytes and embryos from *par*; *par* and *par*; *mex-3* double mutants that were created by injecting double-stranded RNA (dsRNA) specific to one gene into hermaphrodites mutant for a second gene (Fire et al., 1998). In all cases, injection of gene-specific dsRNA into wild-type adults produced a phenotype indistinguishable from that produced by strong loss-of-function alleles (data not shown). While highly penetrant RNAi and/or strong loss-of-function alleles were used for all experiments, there is a possibility that some residual activity remains.

We first examined the genetic relationship between *par-1*, *par-4* and *par-3* with respect to PAL-1 expression. *par-3* mutants express PAL-1 in zero, two or four cells at the four-cell stage, while *par-1* and *par-4* mutants fail to express PAL-1 in the early embryo (Fig. 1B-D, Fig. 2A) (Bowerman et al., 1997). We found that *par-3(RNAi)* embryos did not express

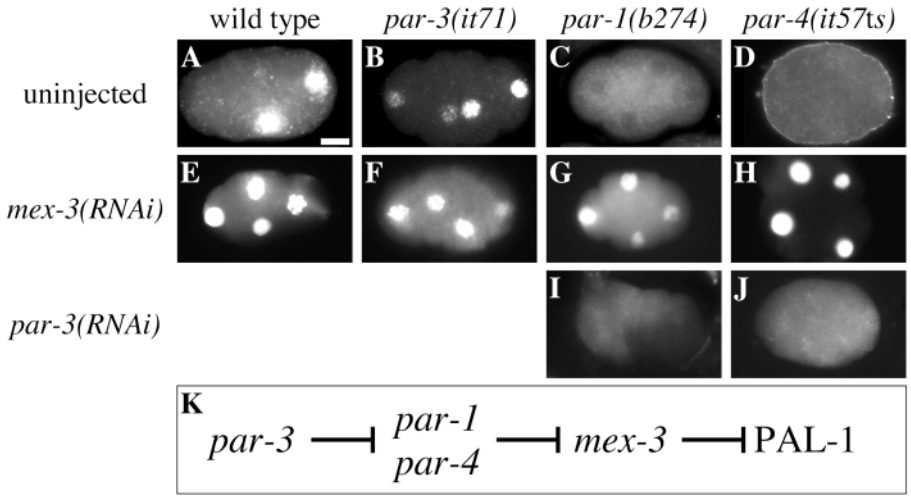

Fig. 1. PAL-1 immunolocalization in *par* and *mex-3* single and double mutant embryos. Strains mutant for the gene indicated above each column were injected with dsRNA as indicated to the left of each row (see Fig. 2A for quantitative summary of staining experiments). (A) Wild-type four-cell embryos express PAL-1 in the two posterior blastomeres. (B) *par-3* embryos express PAL-1 in variable patterns, including in all four blastomeres, as shown. (C) *par-1* and (D) *par-4* embryos do not express PAL-1. (E-H) PAL-1 is expressed in all blastomeres of all double mutants that include *mex-3(RNAi)*. We observed that *par-4; mex-3* embryos often failed to complete early cell cycle events normally, including nuclear division and cytokinesis. (I) *par-1; par-3(RNAi)* embryos and (J) *par-4; par-3(RNAi)* embryos do not express PAL-1. (K) Working model for control of PAL-1 expression. *par-3* restricts *par-1* and *par-4* activities to the posterior, where they inhibit *mex-3* repression of PAL-1. In this and all subsequent figures, embryos are oriented anterior left and dorsal upwards when it is possible to determine polarity. Scale bar: 10 μm.

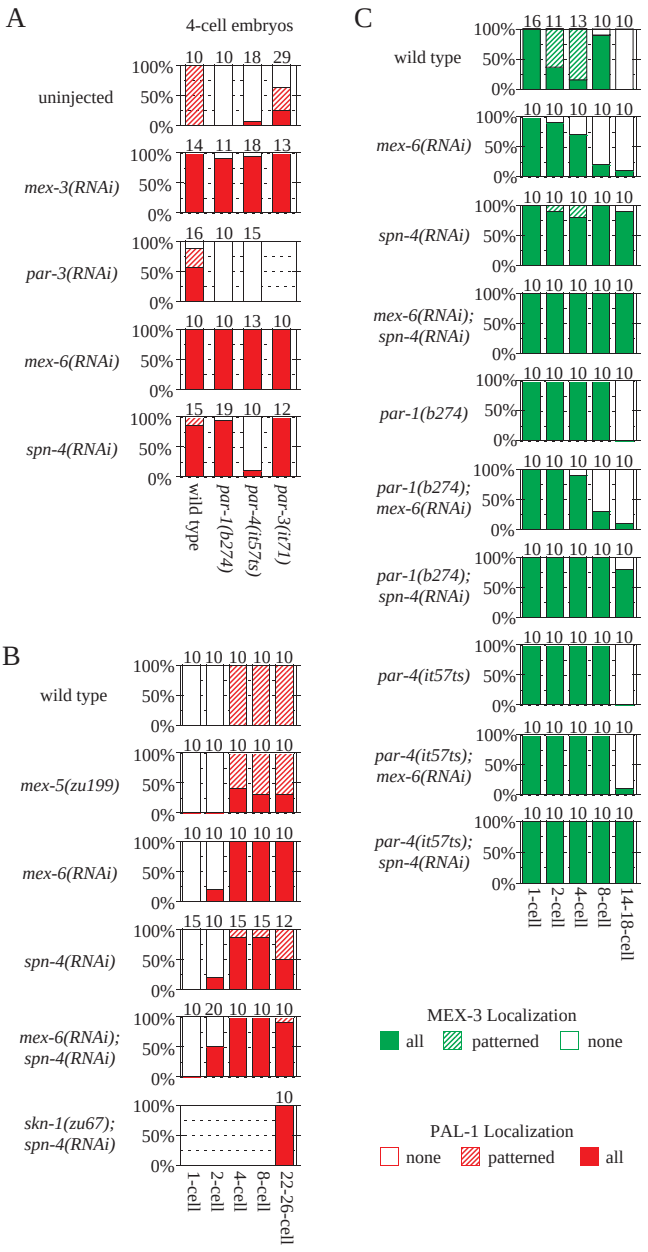

Fig. 2. Quantitative summary of PAL-1 and MEX-3 localization data. (A) PAL-1 localization patterns in four-cell embryos. Wild-type, *par-1*, *par-4* or *par-3* hermaphrodites, as indicated below the graphs, were injected with dsRNA, as indicated on the left. PAL-1 was scored as being present in none of the nuclei, all of the nuclei or patterned (see key). Patterned embryos express PAL-1 only in posterior blastomeres (see Fig. 1A), with the exception of *par-3(it71)* and *par-3(RNAi)* embryos, which express PAL-1 in two of four blastomeres but do not have an obvious polarity. Data for uninjected *par-4(it57*ts*)* and uninjected *par-3(it71)* embryos are taken from Bowerman et al. (Bowerman et al., 1997). (B) PAL-1 localization in embryos at different stages. Genotypes are indicated to the left and embryo stage is indicated below the graphs. In all cases in which PAL-1 was scored as patterned, PAL-1 was expressed only in posterior blastomeres (see Fig. 3B-D). (C) MEX-3 localization in wild-type and mutant embryos at different stages. Genotypes are indicated to the left and embryo stage is indicated below the graphs. In all two- and four-cell embryos in which MEX-3 was scored as patterned, MEX-3 was clearly brighter in the anterior blastomere(s) than in the posterior blastomere(s), as in the wild-type four-cell embryo in Fig. 5A2. In two- and four-cell embryos that were scored as 'all', MEX-3 was detected in all blastomeres with no clear asymmetries in signal intensity between anterior and posterior. Eight-cell and 14- to 18-cell embryos were not scored for MEX-3 patterning and were scored only for the presence or absence of MEX-3 in the majority of blastomeres. In this way, wild-type embryos expressing MEX-3 in P_2 blastomere descendants (see Fig. 5A4) were scored as 'none' because they do not express MEX-3 in the majority of blastomeres. The data presented in these graphs reflect only the presence or absence of MEX-3 and do not reflect the intensity of MEX-3 signal, with the exception of clearly 'patterned' embryos, as described above. The total number of embryos scored is indicated above each bar in each case.

PAL-1 in the absence of *par-1* or *par-4* (Fig. 1I,J, Fig. 2A), suggesting that *par-3* acts genetically upstream of *par-1* and *par-4* for control of PAL-1 expression. This is consistent with published results showing that anterior PAR-3 protein is required to restrict PAR-1 protein to the posterior cortex (Etemad-Moghadam et al., 1995) and may also explain the variable PAL-1 expression patterns observed in *par-3(–)* mutants, as *par-1* and *par-4* activities may be variably distributed in *par-3* mutant embryos.

As *par-1* and *par-4* are required for PAL-1 expression in wild-type and *par-3(–)* embryos, we next asked whether *par-1* and *par-4* are required for PAL-1 expression in *mex-3* mutant embryos. In *par-1; mex-3(RNAi)* and *par-4; mex-3(RNAi)* double mutants, we found that PAL-1 was expressed at high levels in oocytes and all blastomeres (Fig. 1G,H, Fig. 2A), suggesting that *par-1* and *par-4* normally promote PAL-1 expression by inhibiting *mex-3* activity. *par-3; mex-3(RNAi)* double mutants also express PAL-1 in the *mex-3(–)* pattern instead of in variable patterns (Fig. 1F, Fig. 2A). Similar results were obtained with *mex-3; par-1* and *mex-3; par-3* genetic double mutants (data not shown). A working model consistent with these results is presented in Fig. 1K; *par-3* is upstream of *par-1* and *par-4*, both of which are upstream of *mex-3*. It should be noted that this and all subsequent models are based on genetic data and are not intended to indicate direct physical interactions.

Consistent with the proposed model, at the two-cell stage, PAR-1 is enriched in the posterior blastomere that will give rise to all PAL-1-expressing cells (Guo and Kemphues, 1995). Two separate lines of evidence suggest that the spatial pattern of PAL-1 expression is determined at the two-cell stage. First, PAL-1 is detected in the posterior of all wild-type four-cell embryos (Fig. 2A), even if the posterior blastomeres have just completed cytokinesis. This indicates that PAL-1 synthesis begins immediately after division, suggesting that the regulatory machinery that promotes PAL-1 expression is in place before division. Second, four-cell *par-3(–)* embryos express PAL-1 in zero, two or four cells, never one or three cells (Fig. 2A) (Bowerman et al., 1997). The two anterior cells always express PAL-1 at the same level, and the two posterior cells always express PAL-1 at the same level. These observations suggest that the decision to express PAL-1 is made independently in each blastomere at the two-cell stage, even though the result of this decision is not evident until the four-cell stage.

MEX-3 interacting proteins regulate PAL-1 expression

The spatial pattern of MEX-3 localization correlates with the

Table 1. MEX-3 two-hybrid screen results

Number of isolates	Gene	Similarity	Terminal phenotype*	PAL-1†
4	*mex-3*	Two KH domains	Embryonic arrest	All
1	*mex-6*	Two CCCH type zinc fingers	Embryonic arrest	All starting at the four-cell stage
12	*spn-4* (ZC404.8)	RNA recognition motif	Embryonic arrest	All starting at the four-cell stage
1	K07H8.10‡	RNA recognition motif	Undifferentiated cells	All starting at the four-cell stage
2	T04D1.3	GRB2-like SH3 domain	Embryonic arrest	Variable abnormal
20	*pos-1*	Two CCCH type zinc fingers	Embryonic arrest	Variable abnormal
1	B0250.1	Ribosomal protein L8	Undifferentiated cells	Variable abnormal
1	F25B4.2	Pellino	Embryonic arrest	Wild type
2	C17E4.5	RNA recognition motif	Undifferentiated cells	Wild type
1	C43E11.9	RNA-binding domain	Undifferentiated cells	Wild type
1	F40F8.5	Novel	Viable, fertile	n/d
1	K03B4.7	Novel	Viable, fertile	n/d
1	C27H5.3	RNA recognition motif	Viable, fertile	n/d
1	E02D9.1	Protein kinase domain	Viable, fertile	n/d

*Phenotypes of embryos resulting from RNAi (see Materials and Methods). All embryos produced differentiated tissue, except as noted.
†PAL-1 staining in young embryos.
‡K07H8.10(RNAi) showed inconsistent effects from different preparations of dsRNA (see Materials and Methods) and was therefore only minimally analyzed.
n/d, not determined.

pattern of PAL-1 repression in wild-type, *par-1* and *par-4* embryos (Draper et al., 1996; Bowerman et al., 1997). However, *par-3* mutants express PAL-1 in variable patterns at the four-cell stage, despite uniformly high levels of MEX-3 in all cells, indicating that MEX-3 is not sufficient to repress PAL-1 at this stage (Bowerman et al., 1997). To identify additional proteins that regulate PAL-1 expression, we conducted a yeast two-hybrid screen with the N-terminal half of MEX-3 as bait. The screen of 200,000 transformants yielded 14 unique MEX-3 interacting proteins or MIPs (Table 1). Many of these MIPs contain sequence similarity to factors implicated in RNA metabolism, consistent with the putative role of MEX-3 as an RNA-binding protein. We then used RNAi to determine whether any of the identified MIPs are required to regulate PAL-1 expression. Depletion of three of the MIPs, *mex-6*, ZC404.8 and K07H8.10, caused PAL-1 to be expressed in all blastomeres starting at the four-cell stage (Fig. 2B, Fig. 3E-L and data not shown), while depletion of the other MIPs resulted in wild-type or variable PAL-1 expression (Table 1). K07H8.10 (RNAi) showed inconsistent effects from different preparations of dsRNA (see Materials and Methods) and was therefore only minimally analyzed. Our analysis of *mex-6* and ZC404.8 is described in the following sections.

mex-5 and *mex-6* are required for spatial, but not temporal repression of PAL-1

Before being identified as a MIP, *mex-6* was characterized because it shares high sequence identity with *mex-5*, a maternal effect lethal gene that causes cell fate transformations leading to excess muscle when defective (Schubert et al., 2000). *mex-5* and *mex-6* encode 70% identical proteins with two CCCH type zinc fingers, motifs also found in the maternal proteins PIE-1, MEX-1 and POS-1 (Mello et al., 1996; Guedes and Priess, 1997; Tabara et al., 1999). Work by Schubert and colleagues indicates that *mex-5* and *mex-6* have overlapping functions; *mex-6* single mutants are viable, but *mex-5*; *mex-6* double mutants have a more severe phenotype than *mex-5* single mutants. We find that RNAi with full-length *mex-6* results in ectopic PAL-1 in anterior cells at high penetrance, a phenotype not observed in *mex-5* or *mex-6* single mutants (Fig.

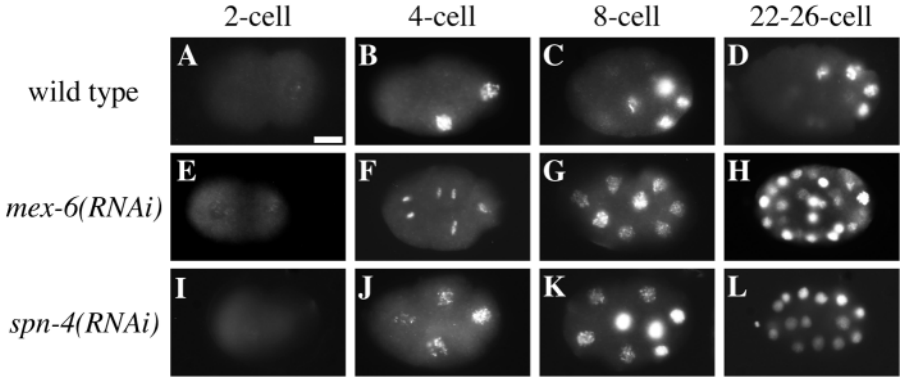

Fig. 3. PAL-1 immunolocalization in wild-type, *mex-6(RNAi)* and *spn-4(RNAi)* embryos. Genotypes and embryo stages are indicated (see Fig. 2B for quantitative summary of staining experiments). (A-D) Wild-type embryos express PAL-1 only in posterior blastomeres starting at the four-cell stage. (E-H) *mex-6(RNAi)* embryos express PAL-1 at equally high levels in all blastomeres starting at the four-cell stage. (F) In the four-cell *mex-6(RNAi)* embryo shown, the two anterior cells are dividing before the posterior cells, demonstrating that *mex-6(RNAi)* embryos can maintain asymmetries in cell cycle time through the four-cell stage. For all 22- to 26-cell embryos, some nuclei are out of the plane of focus. (I-L) *spn-4(RNAi)* embryos express PAL-1 in all blastomeres at the four-cell stage; PAL-1 is often detected at lower levels in anterior blastomeres than posterior blastomeres, as evident in the eight-cell embryo shown (K). Approximately half of (L) *spn-4(RNAi)* 22- to 26-cell embryos express PAL-1 in all blastomeres as shown, the remainder express PAL-1 only in posterior blastomeres, similar to (D) wild-type embryos (see Fig. 2B for quantitation). *spn-4(RNAi)* embryos characteristically maintain asymmetries in cell cycle time as evident in the (K) eight-cell embryo shown, where the anterior blastomeres have proceeded to prophase while the posterior blastomeres are still in interphase.

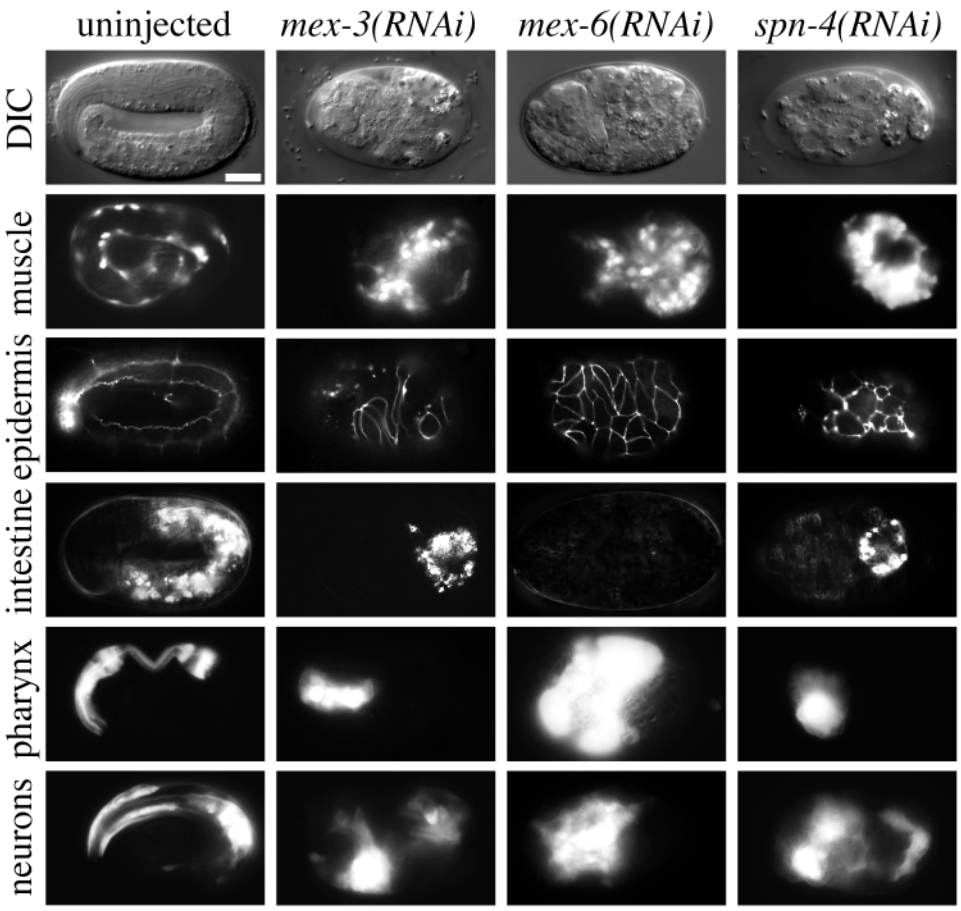

Fig. 4. Terminal phenotypes and cell type abundance in mip(RNAi) embryos. The DIC micrographs in the top row show that *mex-3*, *mex-6* and *spn-4* RNAi embryos produce differentiated cell types but do not undergo morphogenesis. In the remaining rows, body wall muscle, epidermis, intestine, pharynx and neurons were visualized as described in Materials and Methods. *mex-3*, *mex-6* and *spn-4* RNAi embryos produce excess body wall muscle and epidermal cells. *mex-3* and *spn-4* RNAi embryos produce a normal amount of intestine but reduced pharynx, while *mex-6(RNAi)* embryos produce no intestine and excess pharynx. By the time the neural GFP marker was expressed, neural tissue was dispersed throughout the embryo, making it difficult to judge the amount of neural tissue. Thus, we conclude only that neural tissue is present in *mex-3*, *mex-6* and *spn-4* RNAi embryos and do not make any conclusions about the relative amount. For all embryos, some fluorescent signal is out of the plane of focus. This is most noticeable in the intestine micrographs, where the wild-type intestine has elongated but the *mex-3* and *spn-4* RNAi intestine has not.

2B; data not shown). These results suggest that injecting full-length *mex-6* dsRNA reduces the function of both *mex-5* and *mex-6*. Indeed, these genes share extensive regions of nucleotide identity, including seven regions of 30 nucleotides or longer with greater than 90% nucleotide identity, conditions that exceed the minimal requirements for effective gene-specific RNAi (Parrish et al., 2000). Therefore, we interpret our results obtained with full-length *mex-6* dsRNA as reducing the function of both *mex-5* and *mex-6*.

mex-6(RNAi) embryos, like *mex-3(–)* embryos, failed to undergo morphogenesis and produced excess muscle and epidermal cells (Fig. 4). However, *mex-6(RNAi)* embryos also contained an excess of pharyngeal cells and completely lacked gut cells, while *mex-3* mutant embryos produce a reduced number of pharyngeal cells and a normal amount of gut. Like *mex-6(RNAi)* embryos, the genetic *mex-5(zu199)* mutant produces an excess of pharyngeal cells. Curiously, the *mex-6(pk440); mex-5(zu199)* double mutant produces fewer pharyngeal cells (Schubert et al., 2000). These results indicate that *mex-6(RNAi)* may only partially inhibit *mex-5* and that residual *mex-5* or *mex-6* activity may promote pharyngeal development. With the exception of pharynx production, the *mex-6(RNAi)* phenotype appears to be identical to the *mex-6(pk440); mex-5(zu199)* double mutant phenotype (data not shown).

mex-5 and *mex-6* were previously shown to be required for the posterior localization of a number of maternal proteins, including PAL-1 (Schubert et al., 2000). To determine whether *mex-5* and *mex-6* are required for the temporal control of PAL-1 expression, like *mex-3*, or the spatial control of PAL-1 expression, like *par-3*, we stained *mex-6(RNAi)* embryos for PAL-1. We found that *mex-6(RNAi)* disrupts spatial but not temporal control of PAL-1 expression, resulting in embryos that show strong PAL-1 expression in all nuclei starting at the four-cell stage (Fig. 2B, Fig. 3E-H). The ectopic PAL-1 expression in *mex-6(RNAi)* embryos is consistent with the excess muscle and excess epidermis observed, which are fates promoted by the homeodomain protein PAL-1.

spn-4 is required for spatial, but not temporal repression of PAL-1

ZC404.8 encodes an RNA recognition motif (RRM) protein that was also identified as a mutant with defects in spindle rotation, *spn-4*, and as a POS-1 interacting protein, *pip-1* (Gomes et al., 2001) (K. Ogura and Y. Kohara, personal communication). *pos-1*, which was also identified in our two-hybrid screen with MEX-3, encodes a germline-restricted protein containing two CCCH zinc-finger motifs also found in *mex-5* and *mex-6* (Tabara et al., 1999). *spn-4(RNAi)* produced *mex-3*-like embryos that failed to undergo morphogenesis, produced excess muscle, excess epidermal cells, a reduced number of pharyngeal cells and a normal amount of intestine (Fig. 4) (at later times after injection, an increasing proportion of animals fail to differentiate intestine and other tissues – see Materials and Methods).

Starting at the four-cell stage, *spn-4(RNAi)* embryos

consistently showed weak ectopic PAL-1 expression in anterior cells in addition to wild-type PAL-1 expression in the posterior (Fig. 2B, Fig. 3I-L). (See Fig. 3K to compare weak versus strong staining in an eight-cell embryo.) This indicates that *spn-4*, like *mex-5* and *mex-6* and *par-3*, is required for spatial, but not temporal patterning of PAL-1. The ectopic PAL-1 expression in *spn-4(RNAi)* embryos is consistent with the *mex-3*-like terminal phenotype.

mex-5, *mex-6* and *spn-4* have opposite effects on MEX-3 expression levels

To determine whether *mex-5*, *mex-6* and *spn-4* affect MEX-3 expression or activity, we stained *mex-6(RNAi)* and *spn-4(RNAi)* embryos with MEX-3 antibodies. In *mex-6(RNAi)* oocytes and newly fertilized one-cell embryos, MEX-3 was distributed throughout the cell at levels similar to wild type (Fig. 2C and data not shown). However, by the four-cell stage, MEX-3 levels in all blastomeres were lower than is typically seen in wild-type posterior blastomeres (Fig. 5A2,B2). Furthermore, MEX-3 was undetectable by the eight-cell stage, while it is readily detectable throughout wild-type eight-cell embryos (Fig. 2C, Fig. 5A3,B3). These results suggest that the anteriorly localized MEX-5 and MEX-6 proteins (Schubert et al., 2000) (N. N. H. and C. P. H., unpublished) are required to stabilize MEX-3 in the anterior to pattern its expression. If MEX-3 is required at the four-cell stage to repress PAL-1 expression, the ectopic PAL-1 in *mex-6(RNAi)* embryos can be explained solely by the failure to stabilize MEX-3, although we cannot rule out the possibility that *mex-5* and *mex-6* may be directly involved in PAL-1 repression.

By contrast, in young *spn-4(RNAi)* embryos, MEX-3 protein levels appeared higher in all blastomeres than is ever detected in wild type, and in most cases was not clearly patterned (Fig. 2C, Fig. 5C). This indicates that MEX-3 is either not active or is insufficient at the four-cell stage to repress PAL-1 expression in *spn-4(RNAi)* embryos. Furthermore, we found that MEX-3 staining persisted much longer than in wild type. In 14- to 18-cell wild-type embryos, MEX-3 is undetectable except for weak staining in the P_2 blastomere descendants (Fig. 5A4), whereas in *spn-4(RNAi)* embryos, MEX-3 is readily detectable at the 14- to 18-cell stage and in some cases even persists through the 20- to 30-cell stage (Fig. 2C, Fig. 5C4 and data not shown). These results suggest that *spn-4* is required to inhibit MEX-3 accumulation in older embryos.

To determine whether the presence of MEX-3 at the 14- to 18-cell stage actually reflects an overabundance of MEX-3 at the four-cell stage, when PAL-1 expression is perturbed, we used image analysis software to measure the intensity of MEX-3 staining in wild-type and *spn-4(RNAi)* four-cell embryos (Fig. 6A-C). We measured MEX-3 intensity in the anterior blastomere ABa, which normally expresses high levels of MEX-3, and in the posterior blastomere EMS, which normally expresses low levels of MEX-3. In wild-type embryos, we found that ABa was always brighter than EMS (Fig. 6A), reflecting the qualitative differences observed by eye. By contrast, much smaller differences were found in *spn-4(RNAi)* embryos between ABa and EMS, demonstrating that *spn-4* is required to pattern MEX-3 (Fig. 6B).

To determine whether MEX-3 levels were higher in *spn-4(RNAi)* embryos than in wild type, we compared the measured levels between embryos. Although there is considerable variation in the antibody staining, a statistically significant difference was observed between *spn-4(RNAi)* and wild-type ABa blastomeres (Fig. 6C), indicating that *spn-4(RNAi)* embryos do contain an overabundance of MEX-3 at the four-cell stage. The largest difference was observed between *spn-4(RNAi)* and wild-type EMS blastomeres (Fig. 6C), underscoring both the lack of patterning in *spn-4(RNAi)* embryos and the higher overall levels of MEX-3 in *spn-4(RNAi)* embryos. These observations strongly suggest that *spn-4* acts to limit MEX-3 levels and that its activity is preferentially targeted to the posterior blastomeres of four-cell embryos.

These quantitative measurements reflect what we qualitatively observe at the four-cell stage. Furthermore, these data suggest that the persistence of MEX-3 at the 14- to 18-cell stage in *spn-4(RNAi)* embryos does reflect an overabundance of MEX-3 at the four-cell stage. Because of the difficulty in making these measurements, and the relatively large sample sizes required to obtain statistically significant comparisons, all remaining samples were assayed solely for the presence or absence of MEX-3 at the 8- and 14- to 18-cell stages. For all genotypes, the persistence of MEX-3 appeared to correlate with the staining intensity in young embryos.

mex-5 and *mex-6* prevent *spn-4*-dependent degradation of MEX-3

Although *mex-5*, *mex-6* and *spn-4* are required to repress PAL-1 expression in anterior blastomeres, they have opposite effects on MEX-3 expression levels. To determine whether *mex-5* and *mex-6* are required for the abnormal accumulation of MEX-3 observed in *spn-4(RNAi)* embryos, or whether *spn-4* is required for the abnormally low levels of MEX-3 observed in *mex-6(RNAi)* embryos, we stained *mex-6(RNAi); spn-4(RNAi)* double mutant embryos for MEX-3. In the double mutants, MEX-3 persisted through the 14- to 18-cell stage, as in *spn-4(RNAi)* embryos (Fig. 2C, Fig. 5D), suggesting that anterior *mex-5* and *mex-6* (Schubert et al., 2000) (N. N. H. and C. P. H., unpublished) normally act to restrict *spn-4*-dependent degradation of MEX-3 to the posterior. As an indication that the *mex-6* dsRNA was active in these co-injection experiments, MEX-3-stained P-granules were distributed throughout the double mutant embryos as in *mex-6(RNAi)* embryos (see Fig. 5D2).

Despite the persistent MEX-3 staining observed in *spn-4(RNAi)* embryos, PAL-1 is expressed at high levels in the posterior blastomeres and at low levels in the anterior blastomeres. To determine whether *mex-5* and *mex-6* are required for this anterior-posterior asymmetry in PAL-1 expression, we stained *mex-6(RNAi); spn-4(RNAi)* double mutant embryos for PAL-1. In these double mutants, PAL-1 was expressed strongly in all blastomeres (Fig. 2B and data not shown), suggesting that *mex-5* and *mex-6* partially inhibit PAL-1 expression in the anterior of *spn-4(RNAi)* embryos. Consistent with this interpretation, we found that MEX-5 was localized normally to the anterior of two-cell and four-cell *spn-4(RNAi)* embryos (data not shown).

From these results we are able to place *mex-5*, *mex-6* and *spn-4* into a working model for regulation of PAL-1 expression (Fig. 6D). *spn-4* acts to promote MEX-3 degradation while *mex-5* and *mex-6* normally act in the anterior to stabilize MEX-3 and allow it to repress PAL-1.

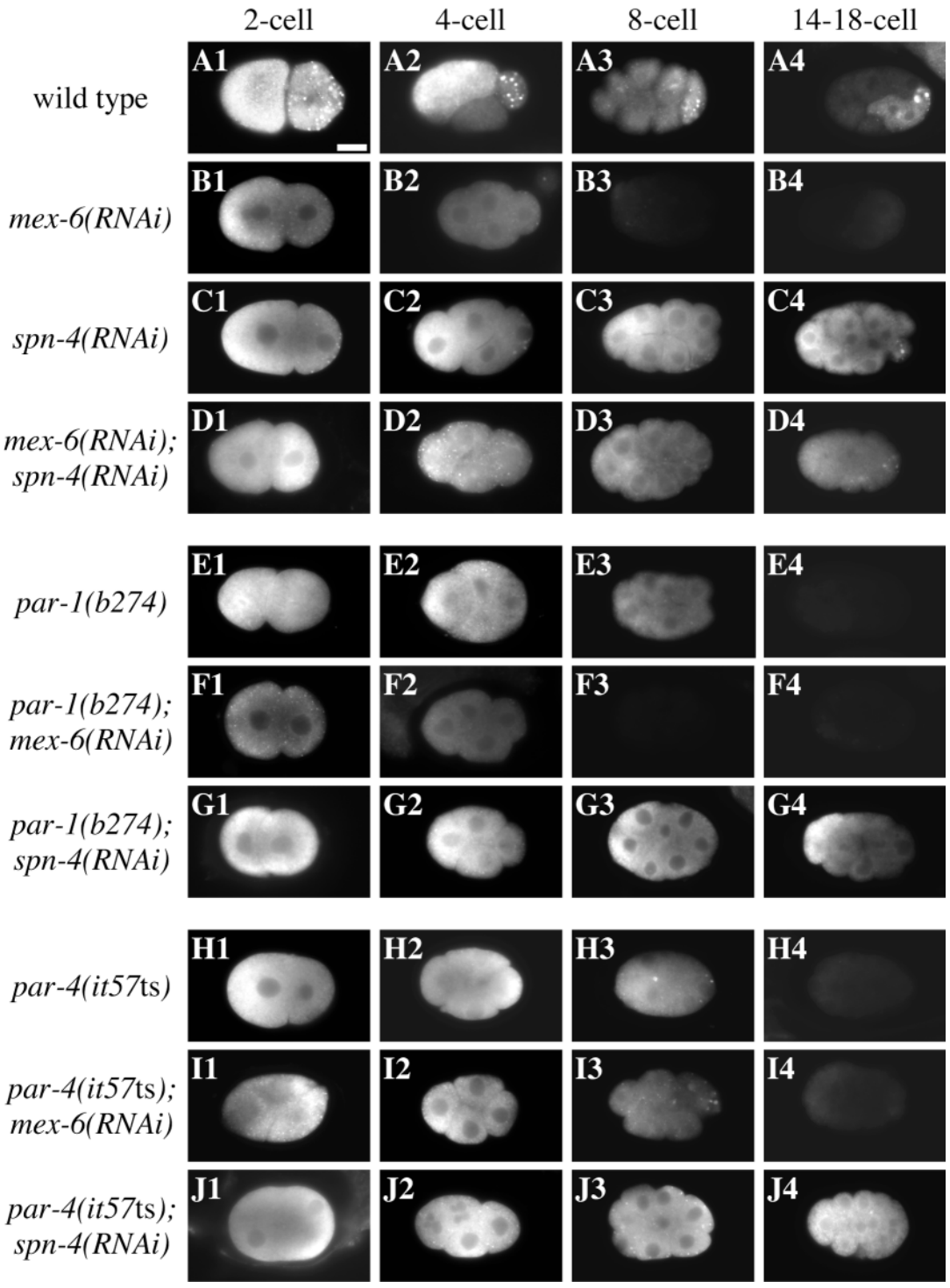

Fig. 5. MEX-3 immunolocalization in wild-type and mutant embryos. Genotypes and embryo stages are indicated (see Fig. 2C for quantitative summary of staining experiments). (A) In wild-type embryos, MEX-3 is present through the eight-cell stage and essentially disappears by the 14- to 18-cell stage, except for weak staining in the P_2 blastomere descendants. (B) In *mex-6(RNAi)* embryos, MEX-3 is undetectable by the eight-cell stage. (C,D) In *spn-4(RNAi)* embryos and *mex-6(RNAi); spn-4(RNAi)* embryos, MEX-3 persists through to the 14- to 18-cell stage. (E) In *par-1* embryos, MEX-3 persists through the eight-cell stage but is undetectable by the 14- to 18-cell stage. (F,G) Defects in *par-1* do not effect the MEX-3 phenotype of *mex-6(RNAi)* embryos or *spn-4(RNAi)* embryos. (H) In *par-4* embryos, MEX-3 persists through the eight-cell stage but is undetectable by the 14- to 18-cell stage. (I) *par-4* is required for the premature degradation of MEX-3 seen in *mex-6(RNAi)* embryos. (J) Defects in *par-4* do not affect the MEX-3 phenotype of *spn-4(RNAi)* embryos. Slight variations in the intensity of MEX-3 signal in the micrographs are often the result of the embryo position in the focal plane, and may not reflect actual asymmetries in protein distribution. Only clear asymmetries that are visible in all focal planes, as in A2, were scored as patterned (see Fig. 2C). Representative embryos are shown. Owing to the high intensity of the signal, (C,D,G,J) *spn-4(RNAi)* two- and four-cell embryos are generally underexposed relative to other embryos. All eight-cell embryos are shown at the same exposure, with the exception of C3 and G3, which are underexposed relative to the other eight-cell embryos. All 14- to 18-cell embryos are shown at the same exposure with the exception of C4, G4 and J4, which are underexposed relative to the other 14- to 18-cell embryos. In two-cell (B1) *mex-6(RNAi)* and (C1) *spn-4(RNAi)* embryos, the anterior cell is typically larger than the posterior cell as in (A1) wild type, demonstrating that *mex-6* and *spn-4* RNAi embryos can maintain asymmetries in cell size. *mex-6(RNAi)* disrupts P-granule localization as monitored by MEX-3 localization to P-granules (Draper et al., 1996). Ten out of 10 *mex-6(RNAi)* embryos mis-segregate P-granules to all blastomeres of the four-cell embryo, while 10/10 of *spn-4(RNAi)* embryos segregate P-granules normally. (D) *mex-6(RNAi); spn-4(RNAi)* double mutant embryos show persistent MEX-3 expression characteristic of *spn-4(RNAi)* embryos, while 8/10 four-cell embryos mislocalize P-granules like *mex-6(RNAi)* embryos, indicating that both injected dsRNAs were effective in RNAi.

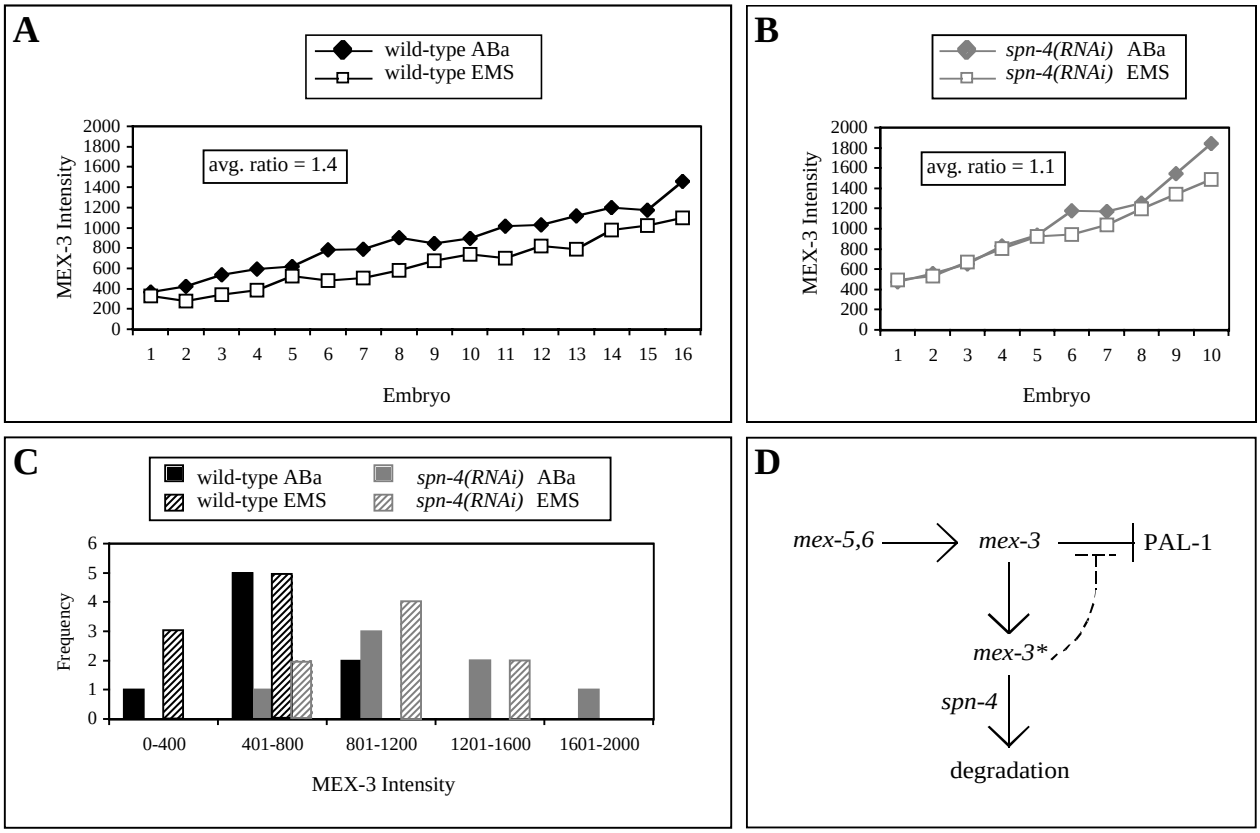

Cell	Mean ± s.d. (n)	Ratio	t-test
spn-4(RNAi) ABa	1101 ± 443 (8)	1.7	P < 0.05
wild-type ABa	645 ± 220 (8)		
spn-4(RNAi) EMS	985 ± 331 (8)	2.1	P < 0.005
wild-type EMS	477 ± 127 (8)		

Fig. 6. MEX-3 intensity and working model. MEX-3 intensity in ABa and EMS from individual (A) wild-type or (B) *spn-4(RNAi)* embryos. The average ratio between ABa and EMS intensities is given. (C) Comparison of MEX-3 intensity in wild-type and *spn-4(RNAi)* blastomeres. Units are arbitrary for MEX-3 intensity. (D) Working model for regulation of PAL-1 expression. MEX-3 exists in active and inactive (*) forms. The active form is normally associated with *mex-5* and *mex-6* and is competent to repress PAL-1. In the absence of *mex-5* and *mex-6*, the inactive form is targeted for degradation by *spn-4*. In the absence of *spn-4*, the inactive MEX-3 accumulates and interferes with active MEX-3.

Based on the observation that MEX-3 is present but inactive in *par-3* and *spn-4(RNAi)* embryos, we suggest that *mex-3* exists in active and inactive forms. The active form is normally associated with *mex-5* and *mex-6* and is competent to repress PAL-1 while the inactive form is normally targeted for degradation by *spn-4*. In the absence of *spn-4*, we propose that inactive MEX-3 accumulates and interferes with active MEX-3, resulting in the weak ectopic PAL-1 expression seen in *spn-4(RNAi)* embryos.

par-3 and *par-1* act upstream of *mex-5, mex-6* and *spn-4*

To determine how *mex-5*, *mex-6* and *spn-4* interact with the par genes that are known to affect PAL-1 expression, we immunostained mip; *par* double mutants for PAL-1. *par-3* embryos express PAL-1 in variable patterns starting at the four-cell stage, while *par-1* and *par-4* embryos fail to express PAL-1 at all in the early embryo (Fig. 2A, Fig. 7A-C). By contrast, *mex-6(RNAi)* and *spn-4(RNAi)* embryos express PAL-1 in all cells at the four-cell stage (Fig. 2A, Fig. 3F,J). We found that PAL-1 was expressed in all mip; *par-3* and mip; *par-1* double mutants (Fig. 2A, Fig. 7D,E,G,H), suggesting that *par-3* and *par-1* function upstream of *mex-5*, *mex-6* and *spn-4* to regulate PAL-1 expression. This is consistent with published results showing that *par-1* is required to localize MEX-5 to the anterior while PAR-1 and PAR-3 are localized normally in *mex-5*(–); *mex-6*(–) embryos (Schubert et al., 2000) and the results indicating that *par-3* is upstream of *par-1*. Furthermore, the characteristic *par-3* cell arrangement (evident in Fig. 7A,D) was often (9/10) suppressed by *spn-4(RNAi)* in *par-3; spn-4(RNAi)* embryos (Fig. 7G), again consistent with *spn-4* acting downstream of *par-3*. Two-cell *par-3(–)* embryos characteristically divide with both spindles oriented anteroposteriorly (Cheng et al., 1995), while two-cell *spn-4* embryos characteristically divide with both spindles oriented dorsoventrally (Gomes et al., 2001).

MEX-3 localization in mip; *par-1* embryos is also consistent with *par-1* acting upstream of *mex-5*, *mex-6* and *spn-4*. *par-1* is not required for the premature degradation of MEX-3 seen in *mex-6(RNAi)* embryos (Fig. 2C, Fig. 5F) or for the excess accumulation of MEX-3 seen in *spn-4(RNAi)* embryos (Fig. 2C, Fig. 5G). This suggests that *mex-5*, *mex-6* and *spn-4* work downstream of or parallel to *par-1* with respect to MEX-3 localization. These data allow us to integrate *par-1*, *par-3*, *mex-*

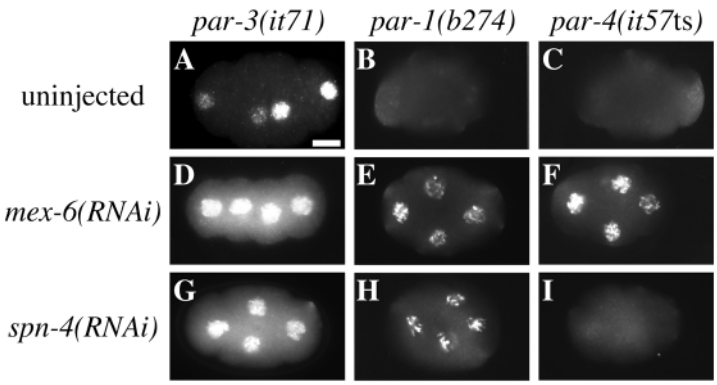

Fig. 7. PAL-1 immunolocalization in *par;* mip(RNAi) double mutant embryos. Strains mutant for the gene indicated above each column were injected with dsRNA (left) (see Fig. 2A for quantitative summary of staining experiments). (A) *par-3* mutants express PAL-1 in variable patterns, including in all four blastomeres, as shown. (B,C) *par-1* and *par-4* mutants do not express PAL-1. (D-F) All double mutants that include *mex-6(RNAi)* express PAL-1 at a high level in all four blastomeres. (G,H) *par-3; spn-4(RNAi)* embryos and *par-1; spn-4(RNAi)* embryos express PAL-1 in all four blastomeres. The characteristic *par-3* cell arrangement (evident in A,D) was suppressed by *spn-4(RNAi)* in 9/10 (G) *par-3; spn-4(RNAi)* embryos. (I) *par-4; spn-4(RNAi)* embryos do not express PAL-1. We observed that *par-4; spn-4(RNAi)* embryos, like *par-4; mex-3(RNAi)* embryos (see Fig. 1), often failed to complete early cell cycle events normally, including nuclear division and cytokinesis.

5, *mes-6* and *spn-4* into one working model for the regulation of PAL-1 expression (Fig. 8B). Anteriorly localized *par-3* restricts *par-1* to the posterior. Posterior *par-1* then restricts *mex-5* and *mex-6* to the anterior, where they stabilize MEX-3 and allow it to repress PAL-1 expression in the anterior. In the absence of *mex-5* and *mex-6* in the posterior, MEX-3 is degraded through a *spn-4*-dependent process.

par-4 analysis indicates that *spn-4* acts in a separate pathway from *mex-5* and *mex-6* to pattern PAL-1

We found that *par-4* activity is not required for PAL-1 expression in *mex-6(RNAi)* embryos (Fig. 2A, Fig. 7F), but *par-4* is required for PAL-1 expression in *spn-4(RNAi)* embryos (Fig. 2A, Fig. 7I), suggesting that *spn-4* acts in a separate pathway from *mex-5* and *mex-6* to control PAL-1 expression. We next looked at MEX-3 expression in mip: *par-4* double mutant embryos. We found that *par-4* is not required for the abnormal persistence of MEX-3 seen in *spn-4(RNAi)* embryos (Fig. 2C, Fig. 5J), but *par-4* is required for the premature degradation of MEX-3 seen in *mex-6(RNAi)* embryos (Fig. 2C, Fig. 5I). We showed earlier that this premature degradation is also dependent on *spn-4* activity, indicating that *par-4* and *spn-4* are both required for MEX-3 degradation in *mex-6(RNAi)* embryos. Furthermore, *par-4* is required for PAL-1 expression in *spn-4(RNAi)* embryos (Fig. 2A, Fig. 7I), suggesting that *par-4* inactivates MEX-3 or a MEX-3 co-factor. We suggest in our working model in Fig. 8B that *par-4* is required to inactivate MEX-3 and target it for *spn-4*-dependent degradation.

spn-4 is required to restrict *skn-1* expression and function

spn-4(RNAi) embryos differ from both *mex-3(–)* and *mex-6(RNAi)* embryos in an important respect; in a large proportion of *spn-4(RNAi)* embryos, PAL-1 expression regresses towards a wild-type pattern. This is particularly evident at the 22- to 26-cell stage when zygotic *pal-1* transcription is thought to begin (Fig. 2B). In wild-type 22- to 26-cell embryos, PAL-1 expression begins to decrease in the EMS descendants relative to the P_2 descendants (Hunter and Kenyon, 1996). In homozygous *pal-1* null embryos from heterozygous mothers, PAL-1 expression in the P_2 descendants begins decreasing at this time as well, indicating that the continued high expression of PAL-1 in the P_2 descendants requires zygotic *pal-1* transcription (Edgar et al., 2001; Hunter and Kenyon, 1996).

Interestingly, PAL-1 zygotic expression appears to require *pal-1* function. The transcription factor SKN-1 inhibits *pal-1* function in the EMS lineage (Bowerman et al., 1993; Hunter and Kenyon, 1996). In 22- to 26-cell *skn-1* mutants, PAL-1 levels remain high in the EMS descendants (C. P. H., unpublished). Thus, the observation that half the *spn-4(RNAi)* embryos expressed PAL-1 in wild-type patterns at the time of maternal to zygotic transition in PAL-1 expression suggests that the ectopic PAL-1 may not be active in half the embryos.

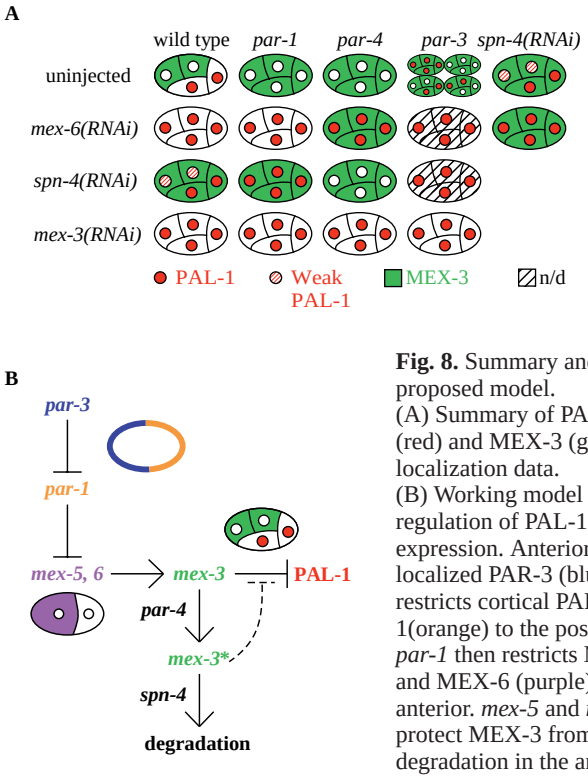

Fig. 8. Summary and proposed model. (A) Summary of PAL-1 (red) and MEX-3 (green) localization data. (B) Working model for regulation of PAL-1 expression. Anteriorly localized PAR-3 (blue) restricts cortical PAR-1(orange) to the posterior. *par-1* then restricts MEX-5 and MEX-6 (purple) to the anterior. *mex-5* and *mex-6* protect MEX-3 from degradation in the anterior, enabling the continued repression of PAL-1. In the absence of *mex-5* and *mex-6* in the posterior, *par-4* inactivates MEX-3 (*), and subjects it to rapid *spn-4*-dependent degradation. In the absence of *spn-4*, inactive MEX-3 can interfere with active MEX-3, resulting in ectopic PAL-1 expression.

One possibility is that SKN-1 may be anteriorly expressed in some *spn-4(RNAi)* embryos and may inhibit the activation of zygotic *pal-1* expression. To test this, we first stained *spn-4(RNAi)* embryos for SKN-1. We found four-cell embryos that expressed SKN-1 predominantly in the two posterior blastomeres, as in wild type (Bowerman et al., 1993), as well as embryos that expressed SKN-1 strongly in all four blastomeres (data not shown). If this anterior SKN-1 can inhibit zygotic PAL-1 expression, then PAL-1 should continue to be expressed in the anterior blastomeres of all *skn-1; spn-4(RNAi)* embryos. Therefore, we injected *skn-1* mutant hermaphrodites with *spn-4* dsRNA and found that, as predicted, all double mutant embryos continued to express PAL-1 in anterior blastomeres through the 22- to 26-cell stage (Fig. 2B). These experiments show that *spn-4* is required to pattern SKN-1 localization and that ectopic SKN-1 inhibits at least some *pal-1* functions.

DISCUSSION

We have identified two proteins, MEX-6 and SPN-4, which are required to pattern PAL-1 expression at the four-cell stage. Our characterization of their genetic interactions with the other factors known to affect PAL-1 patterning, *mex-3, par-1, par-4* and *par-3*, suggests that these two genes couple the spatial and temporal information provided by the par genes to the spatial and temporal pattern of gene expression. Previous work has shown that *mex-3* is required to repress PAL-1 expression and that MEX-3 localization in oocytes and early embryos correlates with the temporal and spatial pattern of PAL-1 repression (Hunter and Kenyon, 1996; Draper et al., 1996). Although the striking correlation between MEX-3 localization and PAL-1 repression is suggestive, in some mutants PAL-1 is expressed in blastomeres that contain high levels of MEX-3 (Bowerman et al., 1997), indicating that MEX-3 activity is regulated independently of expression levels.

Our analysis of *par; mex-3(RNAi)* double mutants suggests that the patterned expression of PAL-1 at the four-cell stage requires PAL-1 repression in oocytes and in one- and two-cell embryos. If PAL-1 is expressed in the oocyte, as it is in *mex-3* mutants, all blastomeres will inherit PAL-1 protein and translationally active *pal-1* RNA, thereby disrupting the spatial regulation of PAL-1 expression. Furthermore, analysis of *par; par-3(RNAi)* double mutants indicates that both *par-1* and *par-4* are required to promote PAL-1 expression at the four-cell stage when *mex-3*-dependent repression is intact. These results also show that *par-3* mutations do not disrupt the regulatory interactions that pattern PAL-1, just their spatial distributions in two-cell embryos. To clarify these interactions and to gain further understanding of how cell polarity information can produce asymmetric patterns of gene expression, we sought to identify additional genes required to pattern PAL-1 expression. As MEX-3 is necessary but insufficient to repress PAL-1 expression, we used a two-hybrid screen to identify MEX-3 interacting proteins and then used RNAi to characterize their functions. By these methods we identified two proteins, SPN-4 and MEX-6, which produced a consistent and informative RNAi phenotype suitable for detailed investigations.

Previous analysis of *mex-5* and *mex-6* indicates that these homologous proteins function redundantly and act downstream of *par-1* to control the asymmetric expression and/or activity of a variety of factors important for early embryogenesis (Schubert et al., 2000). Among these, PAL-1 is the only one for which a specific regulator has been identified, namely MEX-3. We found that *mex-5* and *mex-6* are required for the continued expression of MEX-3 in early embryos and also for continued repression of PAL-1 in anterior blastomeres at the four-cell stage. For both these phenotypes, *mex-6(RNAi)* is epistatic to *par-1(–)*, consistent with the requirement for *par-1* in localizing MEX-5 to the anterior blastomere of two-cell embryos (Schubert et al., 2000). Thus, it appears that MEX-5 and MEX-6 act as adapters to transmit the polarity information conferred by the par genes into the control of PAL-1 expression. As MEX-6 was identified as a MEX-3 interacting protein, one possibility is that MEX-5 and MEX-6 act as co-repressors with MEX-3 at the four-cell stage. Indeed, all double mutants that included *mex-6(RNAi)* express PAL-1 in all blastomeres of four-cell embryos whether MEX-3 is present or not (summarized in Fig. 8A).

A direct interaction between MEX-3 and anteriorly-localized MEX-5 and MEX-6 may also provide a mechanism for maintaining MEX-3 levels in anterior blastomeres. A physical interaction between MEX-5, MEX-6 and MEX-3, or some modification resulting from a physical interaction, could protect MEX-3 from protein degradation. Nevertheless, MEX-5 and MEX-6 are not absolutely required for MEX-3 stability, as MEX-3 is stable in *par-4(–)* and *spn-4(RNAi)* embryos, whether or not *mex-5* and *mex-6* are active. This suggests that *par-4(+)* and *spn-4(+)* may be required to destabilize MEX-3.

In all genetic backgrounds tested, reducing the function of *par-4* or *spn-4* resulted in elevated MEX-3 levels in the posterior, indicating that *par-4* and *spn-4* may normally be required to reduce MEX-3 levels in the posterior. Because PAR-4 and SPN-4 are localized to all cells of two- and four-cell embryos (Watts et al., 2000) (K. Ogura and Y. Kohara, personal communication; N. N. H. and C. P. H., unpublished), their activity must be asymmetrically controlled in the anterior and posterior blastomeres. This difference could be attributed to MEX-5 and MEX-6, which are localized to the anterior and may act to protect MEX-3 from *par-4*- and *spn-4*-dependent degradation.

Despite these similarities, *par-4* and *spn-4* have different effects on PAL-1 expression. In *spn-4(RNAi)* embryos, weak ectopic PAL-1 was detected in anterior blastomeres and normal levels of PAL-1 were detected in posterior blastomeres. Therefore, the abnormally abundant MEX-3 in *spn-4(RNAi)* embryos is either not active or insufficient to repress PAL-1 expression. However, this PAL-1 expression is completely dependent on *par-4* activity. Thus, as in wild-type and *par-3(–)* embryos, *par-4* activity is required to promote PAL-1 expression in *spn-4(RNAi)* embryos. One hypothesis consistent with all the data is that *par-4* activity directly or indirectly inactivates MEX-3. The observation that *par-1* and *par-4* mutations have different effects on PAL-1 expression in *spn-4(RNAi)* embryos provides evidence that *par-1* and *par-4* act by distinct mechanisms to pattern PAL-1 expression at the four-cell stage.

Because PAL-1 expression is dependent on both *par-1* and *par-4*, one attractive hypothesis is that one of these serine/threonine kinases (PAR-1) spatially restricts PAL-1 derepression to the posterior, and the other (PAR-4) temporally

derepresses PAL-1 expression after the two-cell stage. At the two-cell stage, cortically localized PAR-1 is restricted to the posterior blastomere that will give rise to all the PAL-1-expressing cells (Guo and Kemphues, 1995). By contrast, PAR-4 is uniformly localized to both blastomeres at the two-cell stage, suggesting it may be active in temporal regulation (Watts et al., 2000). *par-4* is unique among the par genes in that it is not asymmetrically localized and does not affect asymmetry of the first cleavage (Kemphues et al., 1988), suggesting that it may act later than *par-1* and *par-3*, perhaps providing a temporal cue for early embryonic events including PAL-1 derepression. In this scenario, all blastomeres in four-cell *par-1* mutant embryos execute the fate of anterior blastomeres that do not derepress PAL-1, and all blastomeres in four-cell *par-4* mutant embryos maintain the state of younger blastomeres that do not yet express PAL-1. As *par-3* activity is required for PAR-1 localization (Etemad-Moghadam et al., 1995), *par-3* mutants may variably distribute *par-1* activity, resulting in the variable PAL-1 expression patterns that are observed.

Precedence for separable temporal and spatial control of post-transcriptional gene regulation in *C. elegans* is provided by the analysis of GLP-1 (Evans et al., 1994). *glp-1* mRNA is present throughout the oocyte and early embryo, while GLP-1 protein is expressed only in anterior blastomeres from the two- to 28-cell stage. *cis* regulatory elements have been mapped to two distinct regions in the *glp-1* 3′UTR, with one region being required for temporal control and the other for spatial patterning. As the *pal-1* 3′UTR can confer a PAL-1-like expression pattern on reporter RNAs (Hunter and Kenyon, 1996), PAL-1 expression may be regulated by RNA-binding proteins such as MEX-3 and the MIPs bound to the 3′UTR. In turn, temporal and spatial activity of MEX-3 and the MIPs would ultimately be controlled by the par genes.

These complex genetic interactions are synthesized into a formal genetic model in Fig. 8B in which separate temporal and spatial control pathways converge on MEX-3 to control its activity and stability at the four-cell stage. First, we propose that *par-3* and *par-1* function in a simple linear pathway to localize MEX-5 and MEX-6 to the anterior (Etemad-Moghadam et al., 1995; Schubert et al., 2000) (N. N. H. and C. P. H., unpublished), where they function to stabilize and/or activate MEX-3. This stabilization probably involves direct contact as we identified MEX-6 as a MIP. In addition to stabilizing MEX-3, *mex-5* and *mex-6* are required at the four-cell stage for the continued repression of PAL-1. This is demonstrated by the *par-4; mex-6(RNAi)* and *mex-6(RNAi); spn-4(RNAi)* embryos, which express PAL-1 at high levels in all blastomeres despite abundant MEX-3.

Temporal control of PAL-1 expression may be provided by *par-4(+)* activity. We propose that *par-4* acts directly or indirectly to inactivate MEX-3-dependent repression of PAL-1 at the two- to four-cell stage. The inactivated MEX-3 is then subject to rapid *spn-4*-dependent degradation. *mex-5* and *mex-6* activity in the anterior protects MEX-3 from inactivation and subsequent degradation, thus restricting PAL-1 expression to the posterior. To explain the weak PAL-1 expression in the anterior of *spn-4(RNAi)* embryos, we propose that inactive MEX-3 interferes with active MEX-3. The identification of MEX-3 as a MEX-3 interacting protein (Table 1) is consistent with MEX-3 forming an oligomer. However, we must emphasize that the interactions between MEX-3 and the MIPs were identified in yeast and may not reflect physical interactions in the *C. elegans* embryo.

As *par-4* encodes a serine/threonine kinase, it is tempting to speculate that it may inactivate MEX-3 by directly phosphorylating it. Phosphorylation of KH domain proteins has been shown to affect their RNA binding activity (Wang et al., 1995). Furthermore, phosphorylation is often used to target proteins for degradation (for a review, see Jackson et al., 2000). Finally, MEX-3 is hyperphosphorylated and rapidly degraded in wild-type early embryos (C. P. H., unpublished).

As MEX-3, MEX-5, MEX-6 and SPN-4 all contain RNA-binding motifs, an appealing hypothesis is that these proteins interact on the *pal-1* 3′UTR. However, *mex-3* is the only factor that appears to be specific for regulation of PAL-1 expression; *mex-5* and *mex-6* are required to segregate several unrelated gene products, and *spn-4* is required to control spindle orientation and SKN-1 localization (Draper et al., 1996; Hunter and Kenyon, 1996; Schubert et al., 2000; Gomes et al., 2001) (our data). This raises the possibility of combinatorial control, where MEX-5, MEX-6 and SPN-4 may each act on numerous RNA targets to control their expression, perhaps by regulating the activity and stability of other message-specific *trans*-acting factors similar to MEX-3. The concept of combinatorial control is well documented in transcriptional control, where individual transcription factors can act as activators or repressors of transcription depending on the other factors that are bound (for a review, see Roberts, 2000). Combinatorial control is also emerging as a dominant theme in translational control, but few specific examples are well understood (for a review, see Gray and Wickens, 1998).

Asymmetric protein expression resulting from post-transcriptional regulation is best understood in *Drosophila*. However, *Drosophila* embryos are distinct from nematode and vertebrate embryos because they are polarized before fertilization and begin development as a syncytial blastoderm. This means that maternal RNAs and proteins can be localized during oocyte maturation and that after fertilization, RNA and protein can diffuse freely through the cytoplasm. Perhaps because of these unique characteristics, many factors important for converting polarity cues to asymmetric gene expression during early *Drosophila* development do not have homologs in other systems; two notable exceptions being Caudal/PAL-1 (Macdonald and Struhl, 1986; Waring and Kenyon, 1991) and Par-1 (Guo and Kemphues, 1995; Shulman et al., 2000). In the *C. elegans* embryo, many asymmetrically expressed proteins have been identified, but relatively little is known about how that asymmetric expression is achieved (for a review, see Goodwin and Evans, 1997). The new findings presented in this work provide a framework for understanding how initial cellular polarity can be refined to produce asymmetric gene expression in a cellular system.

We thank J. Gomes, S. E. Encalada, K. A. Swan, C. A. Shelton, J. C. Carter and B. Bowerman for communicating work before publication. We also thank K. Ogura and Y. Kohara for communicating work before publication. We are grateful to C. Schubert and J. Priess for providing anti-MEX-5 antibodies and *mex-5* and *mex-6* mutant strains. We thank J. M. Rihel and A. J. Kay for thoughtful review of this manuscript. This work was supported in part by a March of Dimes Basil O'Connor scholar award (C. P. H.),

National Institutes of Health grant GM 61677 (C. P. H.) and National Institutes of Health grant R01HG01715A1 (M. V.). N. N. H. is partially supported by an NSF predoctoral fellowship.

REFERENCES

Bowerman, B. (1998). Maternal control of pattern formation in early *Caenorhabditis elegans* embryos. *Curr. Top. Dev. Biol.* **39**, 73-117.

Bowerman, B., Draper, B. W., Mello, C. C. and Priess, J. R. (1993). The maternal gene *skn-1* encodes a protein that is distributed unequally in early *C. elegans* embryos. *Cell* **74**, 443-452.

Bowerman, B., Ingram, M. K. and Hunter, C. P. (1997). The maternal *par* genes and the segregation of cell fate specification activities in early *Caenorhabditis elegans* embryos. *Development* **124**, 3815-3826.

Brenner, S. (1974). The genetics of *Caenorhabditis elegans*. *Genetics* **77**, 71-94.

Cheng, N. N., Kirby, C. M. and Kemphues, K. J. (1995). Control of cleavage spindle orientation in *C. elegans*: the role of the genes *par-2* and *par-3*. *Genetics* **139**, 549-559.

Draper, B. W., Mello, C. C., Bowerman, B., Hardin, J. and Priess, J. R. (1996). MEX-3 is a KH domain protein that regulates blastomere identity in early *C. elegans* embryos. *Cell* **87**, 205-216.

Edgar, L. G., Carr, S., Wang, H. and Wood, W. B. (2001). Zygotic Expression of the *caudal* Homolog *pal-1* Is Required for Posterior Patterning in *Caenorhabditis elegans* Embryogenesis. *Dev. Biol.* **229**, 71-88.

Etemad-Moghadam, B., Guo, S. and Kemphues, K. J. (1995). Asymmetrically distributed PAR-3 protein contributes to cell polarity and spindle alignment in early *C. elegans* embryos. *Cell* **83**, 743-752.

Evans, T. C., Crittenden, S. L., Kodoyianni, V. and Kimble, J. (1994). Translational control of maternal *glp-1* mRNA establishes an asymmetry in the *C. elegans* embryo. *Cell* **77**, 183-194.

Fire, A., Xu, S., Montgomery, M. K., Kostas, S. A., Driver, S. E. and Mello, C. C. (1998). Potent and specific genetic interference by double-stranded RNA in *Caenorhabditis elegans*. *Nature* **391**, 806-811.

Goldstein, B. and Hird, S. N. (1996). Specification of the anteroposterior axis in *Caenorhabditis elegans*. *Development* **122**, 1467-1474.

Gomes, J. E., Encalada, S. E., Swan, K. A., Shelton, C. A., Carter, J. C. and Bowerman, B. (2001). The maternal gene *spn-4* encodes a predicted RRM protein required for mitotic spindle orientation and cell fate patterning in early *C. elegans* embryos. *Development* **128**, 4301-4314.

Goodwin, E. B. and Evans, T. C. (1997). Translational control of development in *C. elegans*. *Semin. Cell Dev. Biol.* **8**, 551-559.

Gray, N. K. and Wickens, M. (1998). Control of translation initiation in animals. *Annu. Rev. Cell Dev. Biol.* **14**, 399-458.

Guedes, S. and Priess, J. R. (1997). The *C. elegans* MEX-1 protein is present in germline blastomeres and is a P granule component. *Development* **124**, 731-739.

Guo, S. and Kemphues, K. J. (1995). *par-1*, a gene required for establishing polarity in *C. elegans* embryos, encodes a putative Ser/Thr kinase that is asymmetrically distributed. *Cell* **81**, 611-620.

Hung, T. J. and Kemphues, K. J. (1999). PAR-6 is a conserved PDZ domain-containing protein that colocalizes with PAR-3 in *Caenorhabditis elegans* embryos. *Development* **126**, 127-135.

Hunter, C. P. and Kenyon, C. (1996). Spatial and temporal controls target *pal-1* blastomere-specification activity to a single blastomere lineage in *C. elegans* embryos. *Cell* **87**, 217-226.

Jackson, P. K., Eldridge, A. G., Freed, E., Furstenthal, L., Hsu, J. Y., Kaiser, B. K. and Reimann, J. D. R. (2000). The lore of the RINGS: substrate recognition and catalysis by ubiquitin ligases. *Trends Cell Biol.* **10**, 429-439.

Joberty, G., Petersen, C., Gao, L. and Macara, I. G. (2000). The cell-polarity protein Par6 links Par3 and atypical protein kinase C to Cdc42. *Nat. Cell Biol.* **2**, 531-539.

Kemphues, K. J., Priess, J. R., Morton, D. G. and Cheng, N. S. (1988). Identification of genes required for cytoplasmic localization in early *C. elegans* embryos. *Cell* **52**, 311-320.

Kemphues, K. J. and Strome, S. (1997). Fertilization and establishment of polarity in the embryo. In C. elegans *II* (ed. D. L. Riddle), pp.335-359. Plainview, NY: Cold Spring Harbor Laboratory Press.

Lin, D., Edwards, A. S., Fawcett, J. P., Mbamalu, G., Scott, J. D. and Pawson, T. (2000). A mammalian PAR-3-PAR-6 complex implicated in Cdc42/Rac1 and aPKC signalling and cell polarity. *Nat. Cell Biol.* **2**, 540-547.

Macdonald, P. M. and Struhl, G. (1986). A molecular gradient in early *Drosophila* embryos and its role in specifying the body pattern. *Nature* **324**, 537-545.

Mello, C. C., Schubert, C., Draper, B., Zhang, W., Lobel, R. and Priess, J. R. (1996). The PIE-1 protein and germline specification in *C. elegans* embryos. *Nature* **382**, 710-712.

Parrish, S., Fleenor, J., Xu, S., Mello, C. and Fire, A. (2000). Functional anatomy of a dsRNA trigger: Differential requirement for the two trigger strands in RNA interference. *Mol. Cell* **6**, 1077-1087.

Roberts, G. G. E. (2000). Mechanisms of action of transcription activation and repression domains. *Cell. Mol. Life Sci.* **57**, 1149-1160.

Schubert, C. M., Lin, R., de Vries, C. J., Plasterk, R. H. and Priess, J. R. (2000). MEX-5 and MEX-6 function to establish soma/germline asymmetry in early *C. elegans* embryos. *Mol. Cell* **5**, 671-682.

Shulman, J. M., Benton, R. and St Johnston, D. (2000). The *Drosophila* homolog of *C. elegans* PAR-1 organizes the oocyte cytoskeleton and directs *oskar* mRNA localization to the posterior pole. *Cell* **101**, 377-388.

Siomi, H., Choi, M., Siomi, M. C., Nussbaum, R. L. and Dreyfuss, G. (1994). Essential role for KH domains in RNA binding: impaired RNA binding by a mutation in the KH domain of FMR1 that causes fragile X syndrome. *Cell* **77**, 33-39.

Tabara, H., Hill, R. J., Mello, C. C., Priess, J. R. and Kohara, Y. (1999). *pos-1* encodes a cytoplasmic zinc-finger protein essential for germline specification in *C. elegans*. *Development* **126**, 1-11.

Walhout, A. J. and Vidal, M. (2001). High-throughput yeast two-hybrid assays for large-scale protein interaction mapping. *Methods* **24**, 297-306.

Wang, L. L., Richard, S. and Shaw, A. S. (1995). P62 association with RNA is regulated by tyrosine phosphorylation. *J. Biol. Chem.* **270**, 2010-2013.

Waring, D. A. and Kenyon, C. (1990). Selective silencing of cell communication influences anteroposterior pattern formation in *C. elegans*. *Cell* **60**, 123-131.

Waring, D. A. and Kenyon, C. (1991). Regulation of cellular responsiveness to inductive signals in the developing *C. elegans* nervous system. *Nature* **350**, 712-715.

Watts, J. L., Morton, D. G., Bestman, J. and Kemphues, K. J. (2000). The *C. elegans par-4* gene encodes a putative serine-threonine kinase required for establishing embryonic asymmetry. *Development* **127**, 1467-1475.

Zar, J. J. (1999). *Biostatistical Analysis*. Upper Saddle River, NJ: Prentice Hall.